

## Magnetic-field-induced metal-insulator phenomena in $\text{Pr}_{1-x}\text{Ca}_x\text{MnO}_3$ with controlled charge-ordering instability

Y. Tomioka, A. Asamitsu, H. Kuwahara, and Y. Moritomo  
*Joint Research for Atom Technology (JRCAT), Tsukuba 305, Japan*

Y. Tokura

*Joint Research Center for Atom Technology (JRCAT), Tsukuba 305, Japan  
 and Department of Applied Physics, University of Tokyo, Tokyo 113, Japan*

(Received 17 November 1995)

Field-induced insulator-to-metal transitions have been found in  $\text{Pr}_{1-x}\text{Ca}_x\text{MnO}_3$  ( $0.3 \leq x \leq 0.5$ ) single crystals, which are accompanied by a melting of the insulating charge-ordered (i.e.,  $\text{Mn}^{3+}/\text{Mn}^{4+}$  ordered) state. The transition is of the first order with a hysteresis and is even irreversible at low temperatures. The  $x$ -dependent metal-insulator phase diagrams in the  $H$ - $T$  plane indicate that a deviation of  $x$  from 0.5 modifies the robustness of the charge-ordering state, which is argued in terms of the effect of discommensuration of the charge concentration on the charge-ordered state.

In narrow-band systems, such as  $3d$  transition-metal oxides, the correlation among the charge carriers brings a considerable modification of the electronic properties. In addition to the well-known case of the Mott-Hubbard insulator, the real-space ordering of charge carriers (charge ordering) in a crystal is one of the representative phenomena as a result of the predominant Coulomb interaction over the kinetic energy of the charge carriers. Such a charge-ordering phenomenon has been observed mostly when the concentration of charge carriers takes a rational value of the periodicity of the crystal lattice.<sup>1-4</sup> In addition to the correlation strength among the charge carriers, the commensurability of the carrier concentration with a periodicity of the crystal lattice is thus related to the robustness of the charge-ordered state.

In this paper, we describe the metal-insulator phenomenon induced by a magnetic field in the hole-doped perovskite-type manganese oxide  $\text{Pr}_{1-x}\text{Ca}_x\text{MnO}_3$  ( $0.3 \leq x \leq 0.5$ ). The observed features are relevant to the real-space ordering of 1:1  $\text{Mn}^{3+}/\text{Mn}^{4+}$  species accompanying a lattice structural change and to the magnetic-field-induced melting of such a "charge crystal" state. Although the charge-ordering phenomenon is optimized at  $x = \frac{1}{2}$ , a deviation of  $x$  from  $\frac{1}{2}$  (i.e., discommensuration) weakens the charge-ordered state, which manifests itself as the critically  $x$ -dependent metal-insulator phenomenon under a magnetic field. Since the conduction carriers are strongly coupled with the local spins in terms of double-exchange interaction,<sup>5-7</sup> the resistive state is strongly affected by the local spin state and can be controlled to some extent by an external magnetic field.

Single crystals of  $\text{Pr}_{1-x}\text{Ca}_x\text{MnO}_3$  ( $0.3 \leq x \leq 0.5$ ) were grown by the floating-zone method. The crystal growth was performed in a 100%  $\text{O}_2$  atmosphere at a rate of 3–5 mm/h with rotation of the seed and feed rods in opposite directions. The middle part of the rod was cut out and characterized by the  $x$ -ray Laue and neutron-diffraction measurements, which confirmed the formation of single crystals. The  $x$ -ray powder analysis indicated that all the samples were in a single phase with the orthorhombically distorted perovskite lattice. The orthorhombic distortion was observed to decrease with  $x$  in

accord with results in the literature.<sup>8</sup> The electron-probe microanalysis (EPMA) indicated a nearly identical composition with a prescribed one for each crystal.

Figure 1 shows the electronic phase diagrams of  $\text{Pr}_{1-x}\text{Ca}_x\text{MnO}_3$  crystal (right) and, for comparison, that of  $\text{La}_{1-x}\text{Sr}_x\text{MnO}_3$  crystal (left) (Refs. 9 and 10), which is a prototypical double exchange ferromagnet without charge-ordering instability. The phase diagram of  $\text{Pr}_{1-x}\text{Ca}_x\text{MnO}_3$  has been determined by measurements of the resistivity, magnetization, and neutron diffraction.<sup>11</sup> In  $\text{La}_{1-x}\text{Sr}_x\text{MnO}_3$  the ferromagnetic (fm) metallic state becomes prevailing for

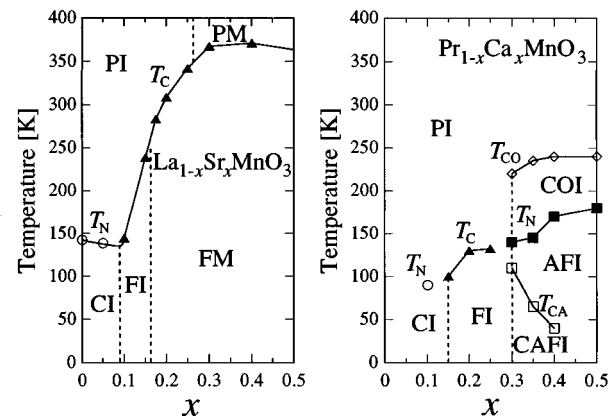


FIG. 1. The magnetic as well as electronic phase diagrams of  $\text{La}_{1-x}\text{Sr}_x\text{MnO}_3$  (Refs. 9 and 10) (left), which is cited from Ref. 10, and  $\text{Pr}_{1-x}\text{Ca}_x\text{MnO}_3$  (right). The PI, PM, and CI denote the paramagnetic insulating, paramagnetic metallic, and canted insulating states, respectively. The FI and FM denote the fm insulating and fm metallic states, respectively.  $T_C$  and  $T_N$  denote the fm Curie and fm Néel temperatures, respectively. For  $0.3 \leq x \leq 0.5$  in  $\text{Pr}_{1-x}\text{Ca}_x\text{MnO}_3$ , the afm insulating (AFI) state exists in the charge-ordered insulating (COI) phase.  $T_{CO}$  and  $T_N$  denote the charge ordering and afm transition temperatures, respectively. The magnetic state for  $T_N < T < T_{CO}$  is paramagnetic. The canted afm insulating (CAFI) state also shows up below the AFI state in the COI phase  $0.3 \leq x \leq 0.4$ .  $T_{CA}$  denotes the canted afm transition temperature.

$x > 0.17$ .<sup>10</sup> Such an appearance of the fm metallic state with an increase in  $x$  (Ref. 12) has been described by the double exchange theory.<sup>5–7</sup> Recent investigations on the magnetotransport property<sup>10,13</sup> have shown that the large negative magnetoresistance (MR) is observed around the fm transition temperature. The application of an external magnetic field reduces the spin scattering in conduction carriers,<sup>14</sup> which is expected to be most pronounced around the Curie temperature  $T_C$ , and hence causes a large negative MR as observed.

On the contrary, a more complex feature appears in the phase diagram of  $\text{Pr}_{1-x}\text{Ca}_x\text{MnO}_3$ : the 1:1 ordering of  $\text{Mn}^{3+}$  and  $\text{Mn}^{4+}$  species (charge ordering) takes place at  $T_{\text{CO}} \approx 230$  K for  $x \geq 0.3$ .<sup>15</sup> The charge-ordering transition accompanied by a change (0.6–2.4 %) in lattice parameters is followed by the antiferromagnetic (afm) and canted afm ordering at lower temperatures ( $< T_{\text{CO}}$ ).<sup>15</sup> By contrast, the fm phase appears at low temperatures for  $0.2 < x < 0.3$ , though the resistivity remains semiconducting even below  $T_C$ . In general, the cations with smaller ionic radii in ( $R, A$ ) sites of  $R_{1-x}A_x\text{MnO}_3$  cause a larger alternating tilting of the  $\text{MnO}_6$  octahedra in a distorted perovskite crystal (of the  $\text{GdFeO}_3$  type) and then a one-electron bandwidth is reduced in a distortion-dependent manner.<sup>16</sup> In the crystal with the reduced one-electron bandwidth, the charge-ordered state tends to show up as observed in  $\text{La}_{1-x}\text{Ca}_x\text{MnO}_3$  ( $x \approx \frac{1}{2}$ ),<sup>17</sup>  $\text{Pr}_{1/2}\text{Sr}_{1/2}\text{MnO}_3$ ,<sup>18,19</sup>  $\text{Nd}_{1/2}\text{Sr}_{1/2}\text{MnO}_3$ ,<sup>20</sup> and also in the present  $\text{Pr}_{1-x}\text{Ca}_x\text{MnO}_3$  crystal.<sup>8,15</sup> The charge-ordered state is expected to be most stabilized when the nominal hole concentration ( $x$ ) takes a commensurate value with the lattice periodicity ( $x = \frac{1}{2}$  in the present case). In  $\text{Pr}_{1-x}\text{Ca}_x\text{MnO}_3$ , however, the charge ordering with the  $(\pi, \pi, 0)$  pattern occurs even for  $x = 0.3$  significantly away from 0.5.<sup>12</sup> The charge and spin ordering for  $0.3 \leq x \leq 0.75$  is basically represented by their afm  $CE$ -type<sup>17</sup> structure of  $\text{Pr}_{0.5}\text{Ca}_{0.5}\text{MnO}_3$ ,<sup>15</sup> where  $\text{Mn}^{3+}$  and  $\text{Mn}^{4+}$  are arranged alternately within the (001) plane, i.e., with the  $(\pi, \pi, 0)$  pattern, and the magnetic lattice is expanded to  $4 \times 4 \times 2$  in the pseudocubic setting.

Figure 2 shows the temperature dependence of resistivity ( $\rho$ - $T$  curve) for  $\text{Pr}_{1-x}\text{Ca}_x\text{MnO}_3$  ( $x = 0.5, 0.4, 0.35$ , and  $0.3$ ) crystals in the absence of a magnetic field and under magnetic fields of 6 and 12 T. The zero-field resistivity is insulating for all the  $x$  values: The  $\rho$ - $T$  curves for  $x = 0.5, 0.4$ , and  $0.35$  show a distinct increase around 220–230 K and that for  $x = 0.3$  shows a small but discernible change in the slope around 200 K, which are all corresponding to the onset of charge ordering. As  $x$  increases toward 0.5, the resistivity anomaly due to the onset of charge ordering becomes clearer. Although the charge ordering for  $x = 0.3$  is barely observed as the small anomaly in the resistivity, a superlattice structure has been confirmed below  $\approx 200$  K as further evidence for the charge ordering by neutron-diffraction measurement.<sup>11</sup>

Application of a magnetic field drastically modifies such an insulating charge-ordered (and in some cases magnetically ordered) state. Let us first see the variation of  $\rho$ - $T$  curves with  $x$  under 6 T. For  $x = 0.5$  the charge-ordering temperature becomes lower than that under zero field and the resistivity remains insulating down to  $T = 0$ . For  $x = 0.4, 0.35$ , and  $0.3$  a similar behavior of  $T_{\text{CO}}$  is seen. However, they show a large resistivity drop by several orders of magnitude at some critical temperature (below 100 K), which indicates

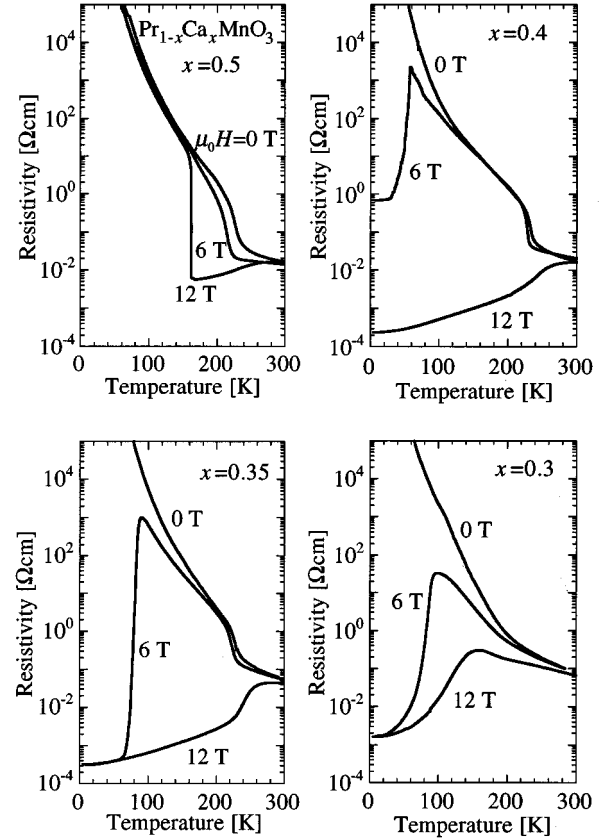


FIG. 2. The temperature dependence of resistivity under  $\mu_0 H = 0, 6$ , and  $12$  T for  $\text{Pr}_{1-x}\text{Ca}_x\text{MnO}_3$  ( $x = 0.5, 0.4, 0.35$ , and  $0.3$ ) crystals. The resistivity was measured in a field cooling (FC) run.

that a charge-ordered state collapses at low temperatures even in case the charge-ordering transition once takes place at a higher temperature.

A further variation with  $x$  appears under 12 T. For  $x = 0.5$  the  $\rho$ - $T$  curve is metallic at high temperatures, but still shows a jump at 160 K, perhaps corresponding to the onset of the charge ordering and the semiconducting behavior persists down to  $T = 0$ . On the contrary, for  $x = 0.4$  and  $0.35$  a trace of charge ordering is completely removed from the resistivity curve and the metallic conduction continues down to low temperatures. Such versatile metal-insulator behaviors as observed in Fig. 2 imply that the deviation of  $x$  from 0.5 plays an important role for a melting of the charge-ordered state from a low-temperature side.

To quantify the observed metal-insulator phenomenon, the isothermal MR was measured for these crystals. Figure 3 exemplifies typical traces of the  $\rho$ - $H$  curves for  $x = 0.35$ . As shown here, the application of a magnetic field causes the transition from the charge-ordered to metallic state with a temperature-dependent hysteresis. Note that a change of the resistivity upon the field-induced transition exceeds several orders of magnitude, in particular, more than ten orders of magnitude at temperatures below 30 K. Furthermore, the hysteresis is pronounced with a decrease in temperature and it becomes so large, e.g., at 4.2 K, that in the field-decreasing process the resistivity no longer recovers to the insulating state. In accord with the metal-insulator phenomenon in  $\rho$ - $H$  curves, the  $M$ - $H$  curve measurements at 30 K showed the

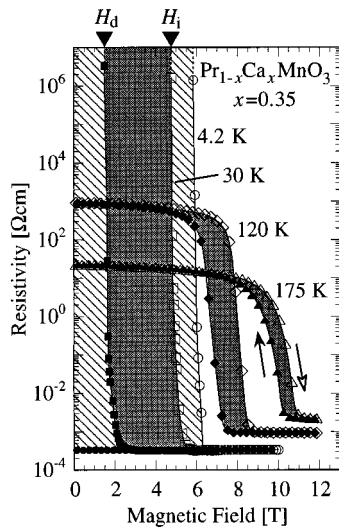


FIG. 3. The  $\rho$ - $H$  curves for the  $\text{Pr}_{1-x}\text{Ca}_x\text{MnO}_3$  ( $x=0.35$ ) crystal taken at 175, 140, 30, and 4.2 K. The hysteresis at 4.2 K is hatched and those at other temperatures are shaded. These isothermal  $\rho$ - $H$  measurements were performed after the sample was cooled to a prescribed temperature under zero field. The magnetic fields where the metamagnetic transitions are observed in the field-increasing and -decreasing runs in the  $M$ - $H$  curve measurements at 30 K are indicated on the upper abscissa as  $H_i$  and  $H_d$ , respectively.

metamagneticlike transition from the canted afm to fm state at  $\approx 5$  T and vice versa at  $\approx 2$  T in the field-increasing and -decreasing runs, respectively, as indicated on the upper abscissa of Fig. 3. Such a resistive transition associated with the magnetic transition from a canted afm to fm state seems to be well in accord with the description of the double-exchange model,<sup>6,7</sup> in which the spin-dependent transfer ( $t$ ) between the neighboring sites is expressed as  $t = t_0 \cos(\Delta\theta/2)$ , where  $\Delta\theta$  is a relative angle of the local  $t_{2g}$  spins and  $t_0$  is the transfer in a fully spin-polarized state.

Figure 4 shows the thus-obtained phase diagrams for  $x=0.5, 0.4, 0.35$ , and  $0.3$ . The hysteretic region is shown by the hatched area. In the case of  $x=0.5$  where the carrier concentration is commensurate, the charge-ordering phase persists down to  $T=0$  at least for  $\mu_0 H \leq 12$  T. In the case of  $x=0.4, 0.35$ , and  $0.3$ , on the other hand, the discommensuration makes the phase boundary shift toward low fields, as shown in Fig. 4, which is pronounced for the lower-temperature region. As another noteworthy aspect of the phase diagram for  $x=0.4, 0.35$ , and  $0.3$ , the hysteresis grows with a decrease in temperature (especially below 20 K). Such a tailing behavior of the phase boundaries toward  $T=0$  may be accounted for in terms of a decrease of the thermal fluctuation effect on the first-order phase transition.<sup>20</sup> Namely, the transition of the metastable state (e.g., field-induced metallic state) is difficult or needs a higher field in case the thermal energy is much less than the potential barrier.

At this stage, the variations of  $\rho$ - $T$  curves with  $x$  as well as with a magnetic field in Fig. 2 are clearly understood in terms of the present metal-insulator phase diagram in the magnetic-field-temperature ( $H$ - $T$ ) plane. The insulator-metal transition was caused from a low-temperature side with increase of field for  $x=0.4, 0.35$ , and  $0.3$ . This is attrib-

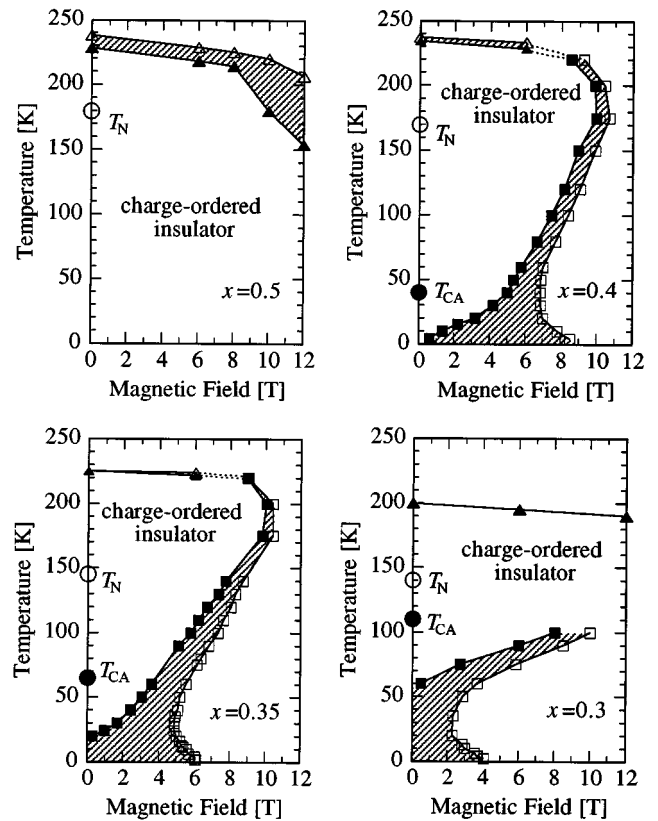


FIG. 4. The phase diagrams in the magnetic-field-temperature plane for the  $\text{Pr}_{1-x}\text{Ca}_x\text{MnO}_3$  ( $x=0.5, 0.4, 0.35$ , and  $0.3$ ). The transition from charge-ordered to not charge-ordered phase is denoted with open squares while that from not charge-ordered to charge-ordered phase is denoted with closed ones. These phase boundaries were determined by the isothermal magnetoresistance (squares) as well as by the resistivity measurements under magnetic field (triangles). The transition magnetic field in the isothermal magnetoresistance measurements is defined as that when the resistivity becomes  $10^{-1} \Omega \text{ cm}$ . The hysteresis is expressed as the hatched area. Zero-field critical temperatures for afm and canted afm transitions are also indicated.

uted to the traversal of the field-cooling (FC) run from the charge-ordered to metallic phase, which is originated from the invasion of the metallic phase in the low-temperature region. In the case of the FC process at 12 T for  $x=0.4$  and  $0.35$ , no trace of charge ordering is seen since the route is out of the corresponding charge-ordered phase.

When a nominal carrier concentration is away from  $x=0.5$ , the afm structure of the charge-ordered state seems to be modified in a critically  $x$ -dependent manner. When  $x$  reduces from 0.5 to 0.3, as an earlier neutron-diffraction study has indicated,<sup>15</sup> the spin arrangement within the  $ab$  plane preserves the  $CE$ -type feature but that along the  $c$  direction changes from antiparallel to parallel. Such an  $x$ -dependent afm structure has been discussed<sup>15</sup> in terms of the double-exchange interaction along the  $c$  direction mediated by the extra electrons, the concentration of which is  $(\frac{1}{2}-x)/\text{Mn}$  site and measures the degree of the discommensuration. Another consequence of discommensuration is that the canted afm state<sup>11</sup> positions lower than the afm state for  $0.3 < x < 0.5$ , as shown in the right panel of Fig. 1. The canting transition temperature decreases with  $x$  approaching 0.5 and as a result

the spontaneous magnetization at 5 K in the canted afm state, which was estimated by extrapolating the  $M$ - $H$  curve ( $1\text{ T} < \mu_0 H < 3\text{ T}$ ) toward  $\mu_0 H = 0$ , decreases with  $x$ , about  $1.7\mu_B/\text{Mn}$  site for  $x=0.3$ ,  $0.2\mu_B/\text{Mn}$  site for  $x=0.4$ . Such critically  $x$ -dependent afm and spin-canting structures seem to be related with the invasion of the metallic phase toward low fields in the low-temperature region for  $x=0.4$ ,  $0.35$ , and  $0.3$ , as shown in Fig. 4.

In summary, we have found the metal-insulator phenomena relating to the collapse of the charge-ordered state, which are either canted afm, afm, or paramagnetic, under magnetic fields in  $\text{Pr}_{1-x}\text{Ca}_x\text{MnO}_3$  ( $0.3 \leq x \leq 0.5$ ). The metal-insulator phase diagrams in the  $H$ - $T$  plane were observed to be critically  $x$  dependent. In particular, the discommensuration of the carrier concentration from the 1:1 ordering of

$\text{Mn}^{3+}:\text{Mn}^{4+}$  species makes the phase boundary shift toward low fields, which is pronounced in a lower-temperature region. As a result, the magnetic-field-induced insulator-to-metal transition is observed to take place irreversibly at low temperatures with a resistivity drop of more than several orders of magnitude, which may be viewed as a different sort of colossal MR phenomenon.

The authors would like to thank H. Kawano and H. Yoshizawa for their neutron-diffraction measurements. The authors are grateful to K. Kishio, K. Kitazawa, H. Akinaga, Y. Yokoyama, and A. Yamada for their help with experiments. This research was supported by NEDO (New Energy and Industrial Technology Development Organization) of Japan, and also by a Grant-In-Aid for Scientific Research from the Ministry of Education, Science and Culture.

- <sup>1</sup>E. J. W. Verwey, P. W. Haaymann, and F. C. Romeijn, *J. Chem. Phys.* **15**, 181 (1941).
- <sup>2</sup>C. H. Chen, S-W. Cheong, and A. S. Cooper, *Phys. Rev. Lett.* **71**, 2461 (1993); S-W. Cheong, H. Y. Hwang, C. H. Chen, B. Batlogg, L. W. Rupp, Jr., and S. A. Carter, *Phys. Rev. B* **49**, 7088 (1994).
- <sup>3</sup>Y. Moritomo, Y. Tomioka, A. Asamitsu, and Y. Tokura, *Phys. Rev. B* **51**, 3297 (1995).
- <sup>4</sup>P. D. Battle, T. C. Gibb, and P. Lightfoot, *J. Solid State Chem.* **84**, 271 (1990).
- <sup>5</sup>C. Zener, *Phys. Rev.* **82**, 403 (1951).
- <sup>6</sup>P. W. Anderson and H. Hasegawa, *Phys. Rev.* **100**, 675 (1955).
- <sup>7</sup>P.-G. de Gennes, *Phys. Rev.* **118**, 141 (1960).
- <sup>8</sup>E. Pollert, S. Krupicka, and E. Kuzmicova, *J. Phys. Chem. Solids* **43**, 1137 (1982).
- <sup>9</sup>G. H. Jonker, *Physica XVI*, 337 (1950); J. B. Goodenough and J. M. Longo, in *Magnetic and Other Properties of Oxides and Related Compounds*, edited by K.-H. Hellwege and A. M. Hellwege, Landolt-Börnstein, New Series, Group III, Vol. 4, Pt. a (Springer-Verlag, Berlin, 1970), p. 126.
- <sup>10</sup>A. Urushihara, Y. Moritomo, T. Arima, A. Asamitsu, G. Kido, and Y. Tokura, *Phys. Rev. B* **51**, 14 103 (1995).
- <sup>11</sup>H. Yoshizawa, H. Kawano, Y. Tomioka, and Y. Tokura, *Phys. Rev. B* **52**, 13 145 (1995).
- <sup>12</sup>G. H. Jonker and J. H. van Santen, *Physica XVI*, 599 (1950).
- <sup>13</sup>Y. Tokura, A. Urushihara, Y. Moritomo, T. Arima, A. Asamitsu, G. Kido, and N. Furukawa, *J. Phys. Soc. Jpn.* **63**, 3931 (1994).
- <sup>14</sup>K. Kubo and N. Ohata, *J. Phys. Soc. Jpn.* **33**, 21 (1972).
- <sup>15</sup>Z. Jirak, S. Krupicka, V. Nekvasil, E. Pollert, G. Villeneuve, and F. Zounova, *J. Magn. Magn. Mater.* **15-18**, 519 (1980); Z. Jirak, S. Krupicka, Z. Simsa, M. Dlouha, and Z. Vratilav, *ibid.* **53**, 153 (1985).
- <sup>16</sup>J. B. Torrance, P. Laccore, A. I. Nazzari, E. J. Ansaldo, and Ch. Niedermayer, *Phys. Rev. B* **45**, 8209 (1992).
- <sup>17</sup>E. O. Wollan and W. C. Koehler, *Phys. Rev.* **100**, 5455 (1955).
- <sup>18</sup>K. Knizek, Z. Jirak, E. Pollert, F. Zounova, and S. Vratilav, *J. Solid State Chem.* **100**, 292 (1992).
- <sup>19</sup>Y. Tomioka, A. Asamitsu, Y. Moritomo, H. Kuwahara, and Y. Tokura, *Phys. Rev. Lett.* **74**, 5108 (1995).
- <sup>20</sup>H. Kuwahara, Y. Tomioka, A. Asamitsu, Y. Moritomo, and Y. Tokura, *Science* **270**, 961 (1995).
- <sup>21</sup>The charge-ordered pattern has been confirmed by the neutron-scattering study (Ref. 8) to be always  $(\pi, \pi, 0)$  over the whole filling range of  $0.3 \leq x \leq 0.5$  in  $\text{Pr}_{1-x}\text{Ca}_x\text{MnO}_3$ . This is contrary to the cases of  $\text{La}_{2-x}\text{Sr}_x\text{NiO}_4$  (Ref. 2) and  $\text{La}_{1-x}\text{Sr}_x\text{FeO}_3$  (Ref. 4) in which the charge ordering is observed at  $x = \frac{1}{3}$  and  $\frac{2}{3}$ , respectively, with the threefold periodicity of the crystal lattice.